Paper

A Study on a Dynamical Aspect of Two or Three Sets of Time Series Data

YOSHINORI NAGAI*, TOSHIO INABA**, and HIROSHI WAKO**

(Recieved January 13, 1995, Revised January 26, 1995)

Abstract: A study is presented to reveal a dynamical aspect of a few sets of time series which show irregular behavior, but which are considered to correlate to each other to some extent. The methods to analyze the time series with a fluctuating nature are discussed from a point of view of deterministic dynamics in comparison with those from a stochastic point of view. As an example, the method using Poincaré sections on an embedding manifold is applied to two or three sets of time series data. The condition is also examined to derive an intrinsic microscopic dynamical aspect from macroscopic time series actually observed.

1. Introduction

In order to study time series it is possible to approach them from two different points of view; that is, stochastic (or statistical) and dynamical ones. If the time series have regular behavior, it is natural to believe that the time series are generated by some deterministic mechanism. On the other hand, if the time series behaved irregularly, it was usual to examine their nature from a statistical point of view, before the existence of deterministic chaos came to our knowledge. Now, we have to examine the time series from a deterministic point of view, even if they show irregular behavior, because deterministic chaos shows stochastic behavior due to its nonlinearity in spite of its deterministic nature.

Many efforts has been devoted by many researchers to analyses of various types of experimental data to check whether they are deterministic chaos or not [1, 2, 3]. However, it is only a few cases that some clear evidences for determinisitic chaos have been found in the experimental data [1, 2, 3]. The number of degrees of freedom of the systems analyzed as deterministic chaos is rather small, usually one degree of freedom.

In this paper we consider how to treat two or three sets of time series data, which are considered to correlate to each other to some extent, so as to reveal their dynamics (or mechanics) behind the observed data. Although the discussion in this paper can be easily extended to more general cases, we confine ourselves to a system with two or three degrees of freedom, i.e., a system that can be described with two or three variables (in other words, we study relationship between two or three sets of time series data from a dynamical point of view). This restriction is convenient for a visual inspection of actual data and calculated results.

*Center for Information Science, and School of Political and Economic Sciences, Kokushikan University
**School of Education and ***School of Social Sciences, Waseda University

In section 2, we discuss stochastic and dynamical aspects of the time series. In physics, it is natural to consider that these two aspects are closely related to each other, because physicists have much interest about causality in observed phenomena. In general, however, these two aspects may be regarded as rather different. This point is discussed by reviewing the methods used in the study on stochastic processes.

Since our main interest in the time series lies in their dynamics, we study the method to obtain an evidence for dynamical causality behind the observed data. In the theory of dynamical systems, a Poincaré section on the manifold constructed by orbits of dynamical variables provides a useful tool. This method is examined in section 3. Some modifications are considered to apply it to several sets of time series data.

In section 4, we show some results of the actual applications to several sets of economic time series data. In this study we used quarterly economic data, which are obtained by properly summing up the base data (i.e., daily or monthly data) during the quarter period. This coarse-graining caused by the summing-up procedure is considered to destroy the deterministic nature in the microscopic level. Hence the influence of the coarse-graining of the microscopic data is discussed. We consider the condition that the intrinsic causality in the microscopic data can be conserved in the macroscopic data actually observed.

Finally, the summary and discussion about the problems remaining are given in section 5.

2. Stochastic Aspect and Dynamical Aspect

Stochastic Aspect

Let us consider a set of time series data $\{x_0, x_1, x_2, \cdots, x_n\}$ (shortly denoted by $\{x_i\}_n$). When this set of time series data has irregular nature, it can be characterized by a probability density or probability distribution, $\{P(x)\}$. The Fourier transformation of $\{P(x)\}$,

$$\phi(s)=\int e^{ixs}P(x)\,dx \tag{2.1}$$

is called characteristic function, where s is a parameter. A logarithm of $\phi(s)$ can be expressed by a cummurant expansion [4, 5]. The cummurants are obtained from the moments of time series data [4, 5].

Now we consider two sets of time series data $\{x_i\}_n$ and $\{y_i\}_n$ whose probability distributions are given as $\{P(x)\}$ and $\{P(y)\}$, respectively. We introduce two-variable probability distribution $\{P(x, y)\}$ for $\{x_i, y_i\}_n$. If the two sets of time series data are independent from each other, the probability distribution $\{P(x, y)\}$ can be expressed as the product of $P(x)$ and $P(y)$, i.e., $\{P(x, y)\}=\{P(x)P(y)\}$. It is interesting to consider the distribution difference of the above two probability distributions;

$$D(x, y)=P(x, y)-P(x)P(y). \tag{2.2}$$

The moments for the distribution difference are given as follows;

$$\langle x^m \rangle_D = \int x^m D(x, y)\, dx\, dy \tag{2.3}$$

$$\langle y^l \rangle_D = \int y^l D(x, y)\, dx\, dy \tag{2.4}$$

$$\langle x^m y^l \rangle_D = \int x^m y^l D(x, y)\, dx\, dy. \tag{2.5}$$

If all the cross moments (2.5) vanish, the two sets of time series data are mutually independent. To the contrary, the existence of non-zero cross moments implies that the two sets of time series, $\{x_i\}_n$ and $\{y_i\}_n$ have some correlation to each other. In the case of $n=l=1$, the cross moment $\langle xy \rangle_D$ for the distribution difference is equivalent to the cross correlation of the two sets of time series data as shown in the following:

$$\begin{aligned}\langle xy \rangle_D &= \int xyD(x, y)\, dx\, dy \\ &= \int xyP(x, y)\, dx\, dy - \int xyP(x)P(y)\, dx\, dy \\ &= \int xyP(x, y)\, dx\, dy - \int x \int P(x, y')\, dx\, dy' \int y \int P(x', y)\, dx'\, dy \\ &= \langle xy \rangle - \langle x \rangle \langle y \rangle. \end{aligned} \tag{2.6}$$

$\langle xy \rangle_D$ devided by the standard deviations s_x and s_y of the distributions $\{P(x)\}$ and $\{P(y)\}$ is a correlation coefficient. The correlation coefficient has a meaning how the two sets of time series data are correlated to each other. For example, if it is equal to one, they have a linear relationship to each other. The cross correlation is usually used in the analysis of time series data from a statistical point of view.

So far, we have considered the time series from only a statistical point of view; in other words, there is no consideration about time or dynamics. If anyone wants to take into account temporal development of the time series in the analysis from a statistical point of view, it is necessary to examine the time series as a stochastic process. In such a treatment, the transition probability, $w(\boldsymbol{x}, t; \boldsymbol{x}', t')$, plays an important role. The chain of the transition probabilities corresponding to a sample path gives a full detail of the dynamics. The chain of the transition probabilities usually expressed as a master equation or the Chapman-Kolmogorov equation,

$$w(\boldsymbol{x}, t; \boldsymbol{x}', t') = \int d\boldsymbol{x}'' w(\boldsymbol{x}, t; \boldsymbol{x}'', t'') w(\boldsymbol{x}'', t''; \boldsymbol{x}', t'). \tag{2.7}$$

When we take into consideration the temporal development in the analysis of the time series, the main problem is how to determine the transition probabilities from the actual time series data under the assumption of Markovian stochastic process. The Fokker-Planck equation, which is a special case of the differential Chapman-Kolmogorov equation called by Gardiner (p. 51 in ref. 4), is one of the answers to this problem. Following the reference 4 (pp. 47–51), we briefly describe the derivation of the differential Chapman-Kolmogorov equation below.

Let the time evolution of an expectation value of a physical quantity $f(\boldsymbol{x})$ be given by the following equation:

$$\langle f(\boldsymbol{x})\rangle(t)=\int \mathrm{d}\boldsymbol{x} f(\boldsymbol{x}) w(\boldsymbol{x}, t; \boldsymbol{x}_0, t_0) \tag{2.8}$$

where $\boldsymbol{x}_0$ and t_0 are an initial position and initial time of the stochastic process, respectively. The differentiation of the expectation value $\langle f(\boldsymbol{x})\rangle(t)$ with respect to time t leads to the differential Chapman-Kolmogorov equation for the transition probability $w(\boldsymbol{x}, t; \boldsymbol{x}', t')$, i.e.,

$$\begin{aligned}\frac{\partial}{\partial t}\langle f(\boldsymbol{x})\rangle(t)&=\int \mathrm{d}\boldsymbol{x} f(\boldsymbol{x}) w(\boldsymbol{x}, t; \boldsymbol{x}_0, t_0)\\ &=\lim_{\Delta t\to 0}\frac{1}{\Delta t}\left\{\int \mathrm{d}\boldsymbol{x} f(\boldsymbol{x})[w(\boldsymbol{x}, t+\Delta t; \boldsymbol{x}_0, t_0)-w(\boldsymbol{x}, t; \boldsymbol{x}_0, t_0)]\right\}\\ &=\lim_{\Delta t\to 0}\frac{1}{\Delta t}\left\{\int \mathrm{d}\boldsymbol{x}\int \mathrm{d}\boldsymbol{x}' f(\boldsymbol{x}) w(\boldsymbol{x}, t+\Delta t; \boldsymbol{x}', t) w(\boldsymbol{x}', t; \boldsymbol{x}_0, t_0)\right.\\ &\quad\left.-\int \mathrm{d}\boldsymbol{x} f(\boldsymbol{x}) w(\boldsymbol{x}, t; \boldsymbol{x}_0, t_0)\right\}\end{aligned} \tag{2.9}$$

Expansion of $f(\boldsymbol{x})$ around $\boldsymbol{x}'$

$$\begin{aligned}f(\boldsymbol{x})=f(\boldsymbol{x}')&+\sum_i \frac{\partial f(\boldsymbol{x})}{\partial x_i'}(x_i-x_i')+\sum_{i,j}\frac{1}{2}\frac{\partial^2 f(\boldsymbol{x})}{\partial x_i'\partial x_j'}(x_i-x_i')(x_j-x_j')\\ &+|\boldsymbol{x}-\boldsymbol{x}'|^2 R(\boldsymbol{x}, \boldsymbol{x}')\end{aligned} \tag{2.10}$$

and substitution of (2.10) into (2.9) leads to the differential Chapman-Kolmogorov equation

$$\begin{aligned}w(\boldsymbol{x}' t; \boldsymbol{x}_0, t_0)=&-\sum_i \frac{\partial}{\partial x_i'}[A_i(\boldsymbol{x}', t) w(\boldsymbol{x}', t; \boldsymbol{x}_0, t_0)]\\ &+\sum_{i,j}\frac{1}{2}\frac{\partial^2}{\partial x_i'\partial x_j'}[B_{ij}(\boldsymbol{x}', t) w(\boldsymbol{x}', t; \boldsymbol{x}_0, t_0)]\\ &+\int \mathrm{d}\boldsymbol{x}[W(\boldsymbol{x}'; \boldsymbol{x}, t) w(\boldsymbol{x}, t; \boldsymbol{x}_0, t_0)-W(\boldsymbol{x}; \boldsymbol{x}', t) w(\boldsymbol{x}', t; \boldsymbol{x}_0, t_0)]\end{aligned} \tag{2.11}$$

The following conditions are used in this derivation

$$\lim_{\Delta t\to 0} w(\boldsymbol{x}, t+\Delta t; \boldsymbol{x}', t)/\Delta t = W(\boldsymbol{x}; \boldsymbol{x}', t) \tag{2.12}$$

(uniformly in $\boldsymbol{x}$, $\boldsymbol{x}'$, and t for $|\boldsymbol{x}-\boldsymbol{x}'|\geqq\varepsilon$)

$$\lim_{\Delta t\to 0}\frac{1}{\Delta t}\int \mathrm{d}\boldsymbol{x}(x_i-x_i') w(\boldsymbol{x}, t+\Delta t; \boldsymbol{x}', t)=A_i(\boldsymbol{x}', t)+\mathrm{O}(\varepsilon) \tag{2.13}$$

$$\lim_{\Delta t\to 0}\frac{1}{\Delta t}\int \mathrm{d}\boldsymbol{x}(x_i-x_i')(x_j-x_j') w(\boldsymbol{x}, t+\Delta t; \boldsymbol{x}', t)=B_{ij}(\boldsymbol{x}', t)+\mathrm{O}(\varepsilon) \tag{2.14}$$

(integration in $|\boldsymbol{x}-\boldsymbol{x}'|<\varepsilon$)

and

$$|R(\boldsymbol{x}, \boldsymbol{x}')|\to 0 \text{ as } |\boldsymbol{x}-\boldsymbol{x}'|\to 0 \tag{2.15}$$

Here it should be noticed that

$$\int \mathrm{d}x f(x) w(x, t; x_0, t_0) = \lim_{\Delta t \to 0} \int \mathrm{d}x \int \mathrm{d}x' f(x') w(x, t+\Delta t; x', t) w(x', t; x_0, t_0) \quad (2.16)$$

In the case that the last term in (2.11) can be neglected, the differential Chapman-Kolmogorov equation is reduced to the Fokker-Planck equation:

$$\frac{\partial}{\partial t} w(x', t; x_0, t_0) = -\sum_i \frac{\partial}{\partial x_i} [A_i(x', t) w(x', t; x_0, t_0)] + \frac{1}{2} \sum_{i,j} \frac{\partial^2}{\partial x_i' \partial x_j'} [B_{ij}(x', t) w(x', t; x_0, t_0)] \quad (2.17)$$

Following the above derivation of the Fokker-Planck equation, we can obtain a procedure to construct a model of stochastic process from the time series, even if the derivation is carried out under some restrictions. The procedure described below, therefore, gives an approximate scheme for the time series. The scheme of the Fokker-Planck equation should be true if the time series satisfy the condition of stationary Markovian process.

Equations (2.13) and (2.14) imply that the mean value and the cross correlation calculated from the time series data have small deviations, while the mean value and the cross correlation can be obtained from the time series data in the situation that small errors are acceptable. Using these mean value and cross correlation, the transition probabilities are given with the solution of the Fokker-Planck equation (2.17). Hence the procedure to make a model of stochastic process becomes as follows:

$$A_i(x', t) \simeq \frac{1}{N_\varepsilon(x)} \sum_k (x_i(k) - x_i') \theta_k(\varepsilon, x(k), x') \quad (2.18)$$

$$B_{ij}(x', t) \simeq \frac{1}{(N_\varepsilon(x))^2} \sum_k (x_i(k) - x_i')(x_j(k) - x_j) \theta_k(\varepsilon, x(k), x') \quad (2.19)$$

$$\theta_k(\varepsilon, x(k), x') = \theta(\varepsilon - \sqrt{\sum_i (x_i(k) - x_i')^2}) \quad (2.20)$$

$$N_\varepsilon(x') = \sum_k \theta_k(\varepsilon, x(k), x') \quad (2.21)$$

where $\{x(k)\}$ means time series data and $\theta(\cdots)$ denotes a step function. Substituting (2.18) and (2.19) into the Fokker-Planck equation (2.17), the solution $\{w(x', t; x_0, t_0)\}$ gives probability distributions for a stochastic process by which the time series data $\{x(k)\}$ are generated.

Dynamical Aspect

The discovery of deterministic chaos have brought about the situation that an irregular nature of time series data is considered to be a result of nonlinear deterministic dynamics. Many works have been carring out along such a line.

It is well known that chaotic orbits (or trajectories) become less predictable as time goes on, but that the manifold constructed by chaotic orbits is stable (this stability called robust). This fact was pointed out at first by Lorenz [6]. In the analysis of time series data from a point of view of chaotic dynamics, the time delayed coordinate embedding method of a few sets of time series is applicalbe [7, 8, 9] owing to robustness of strange attractor of chaotic or-

bits [1, 2, 3]. Most studies of the time series data by the embedding method are carried out for one set of time series data, while embedding of orbits is always possible for any number of sets of the time series data.

Embedding of orbits (or trajectories) into the d-dimensional space shows a manifold in the d-dimensional space. If the manifold constructed by the embedded orbits has a deterministic character, subsections of the manifold are related to each other. A Poincaré section is a kind of subsections. The relation between the subsections is described by a mapping between elements of subsections. This is a useful procedure to study the deterministic relationships between orbits generated in a deterministic dynamical system. Hence it becomes obvious how we can see the determinisity of time series data. The embedded manifold of the time series data is obtained by replacing the continuous orbits with the descrete time series data. Then we see the structure of the embedded manifold and relationships among any sets of time series data.

There exist other situations to see the determinisity of the time series data. As mentioned above, determinisity discussed in this paper is equivalent to the relationship or the mapping between pairs of data points. If we find the mapping

$$f_k: \boldsymbol{u}_i \rightarrow \boldsymbol{u}_{i+k} \tag{2.22}$$

for vector time series data $\{\boldsymbol{u}_i\}_n$, the determinisity of the time series $\{\boldsymbol{u}_i\}_n$ can be described by this mapping; that is, we can reveal the causality of the time series from the mapping (2.22). For one-dimensional time series data the mapping f_k is called return map. It is hard, however, to find such mapping in the actual time series data in most cases. There are many reasons for the difficulties. Unknown dimension to describe the temporal development of the time series is one reason. Another is the stochasticity caused in the observation. This is the reason why the statistical method is used in a practical analysis of the time series data to find the mapping f_k of (2.22); for example, introducing an ensemble $\{\boldsymbol{u}_i\}_{\boldsymbol{u}^*\pm\varepsilon}$ (data collected near the data point $\boldsymbol{u}_i$ within the distance ε), f_k is estimated as an average of ensemble $\{\boldsymbol{u}_{i-k}\}_{\boldsymbol{u}^*\pm\varepsilon}$. The statistical method stated here is very similar to that appearing in the procedure of stochastic processes.

The mapping f_k obtained above reflects a local property of the time series data. If the mapping f_k is equivalent to any other mapping $f_k': \boldsymbol{u}_j \rightarrow \boldsymbol{u}_{j-k} (j=1, 2, \ldots)$, the mapping f_k is called universal. Any information about the time series is obtainable from the mapping f_k. Any mapping that belongs to the same universal mapping undergoes the same kind of causality governing the system.

3. Embedded Manifold and Poincaré Section

Since a strange attractor of chaotic orbits (or trajectories) has the nature of robustness, it is better to analyze the time series data by the embedding method [7, 8]. In this section we briefly review the embedding method to construct the manifold and a Poincaré section to analyze the embedded manifold. In this section, $\{X_i\}_n$, $\{Y_i\}_n$, and $\{Z_i\}_n$ are used for the

time series data and x_i, y_i, and z_i for the variables on the Poincaré section.

Let $\{X_i\}_n$, $\{Y_i\}_n$, and $\{Z_i\}_n$ be three sets of time series data. As mentioned in section 2, the embeded manifold is obtained by embedding three-dimensional vector time series $\{\boldsymbol{u}_i\}_n = \{(X_i, Y_i, Z_i)\}_n$ into d-dimensional space. For convenience sake of our visual inspection we consider the case of $d \leqq 3$. In this explanation we put $d=3$. In such a case, the embedded manifold of the vector time series data is the distribution of data points $\{\boldsymbol{u}_i\}_n$ expressed as

$$\{\sum_i \delta(X-X_i)\delta(Y-Y_i)\delta(Z-Z_i)\}, \tag{3.1}$$

where $\delta(...)$ means a Dirac's delta function. The examples of embedded manifolds for the time series f Lorenz model (Fig. 1) are shown in Fig. 2.

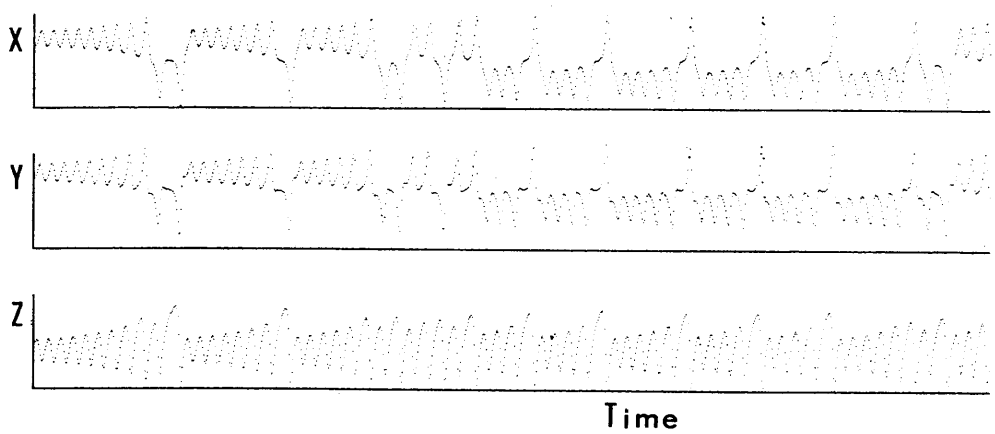

Fig. 1 Time Series Data of Lorenz Model

The ordinary differential equations, $\dot{X}=-cX+cY$, $\dot{Y}=rX-Y+XY$, and $\dot{Z}=XY-bZ$ are solved numerically using the Runge-Kutter method with the parameter values $r=28$, $c=10$, and $b=8/3$.

In order to examine the determinisity of the time series data, a Poincaré section of the embedded manifold and the return maps on the Poincaré section are useful. For simplicity, we consider the Poincaré section on only the planes parallel to either XY-, YZ- or ZX-plane. Although this is slightly different from the ordinary treatment, the difference brings no trouble in the analysis. In Fig. 3 a Poincaré section is illustrated for some fixed Z value. The structure of the embedded manifold is understood by intersection points on the Poincaré section. Let x_i, x_{i+1}, x_{i+2},... and y_i, y_{i+1}, y_{i+2},... be intersection points and t_i, t_{i+1}, t_{i+2},... be intersection times. The return maps representing the relationships between intersection points (x_i, x_{i+1}) and (y_i, y_{i+1}) and between time intervals $(t_{i+1}-t_i, t_{i+2}-t_{i+1})$ are significant for the analysis.

In Fig. 4 some examples of a Poincaré section and return maps on the Poincaré section are shown for the Lorenz model. The determinisity clearly appears in both the Poincaré section and the return maps of intersection points, although the recognition of the structures in these figures is somehow subjective. In the present stage of chaos study, however, such an in-

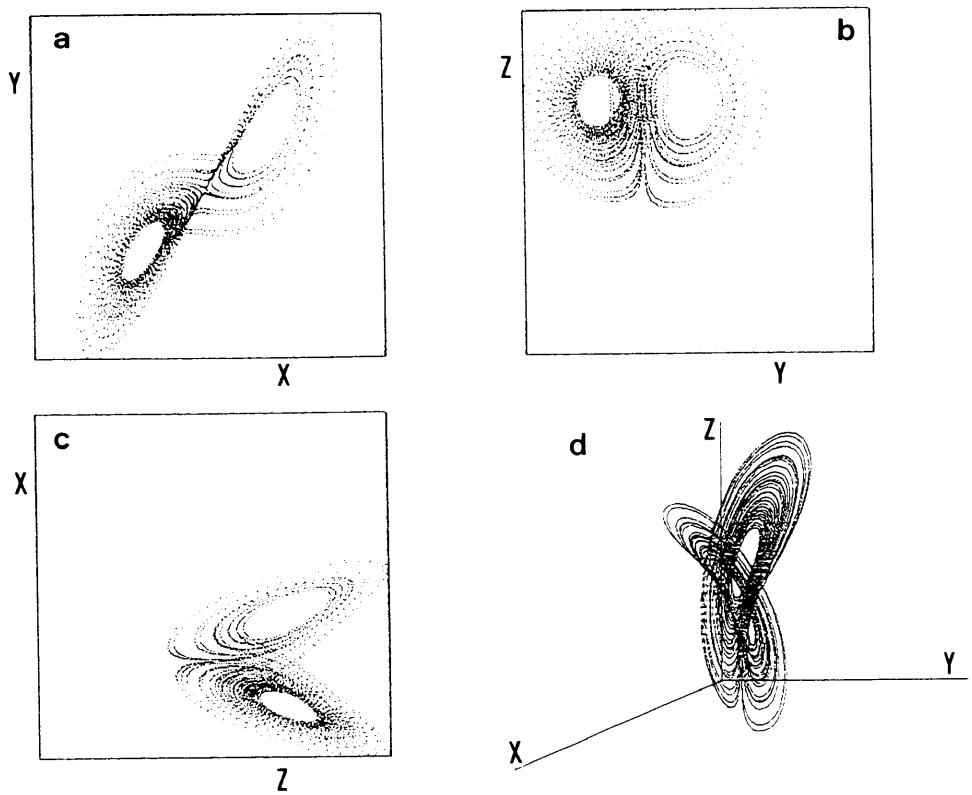

Fig. 2 Embedded Manifolds for the Lorenz Model

a, b, and c are embedded manifolds in the two-dimensional space, and d is the embedded manifold in the three-dimensional space.

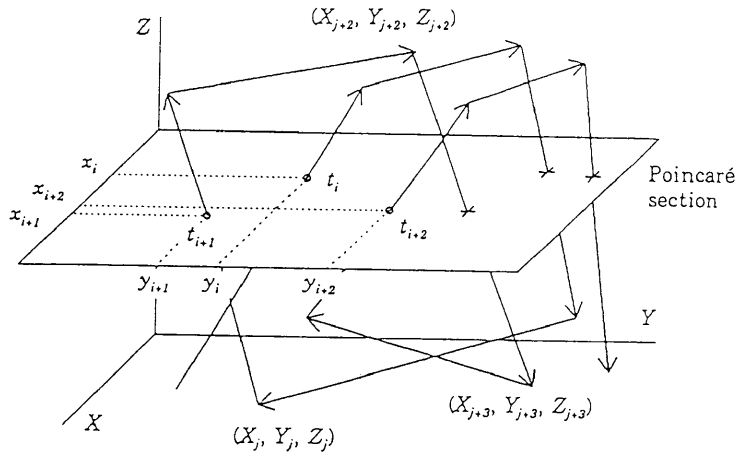

Fig. 3 Schematic Representation of Poincaré Section

The trajectory (or orbit, shown by long arrows) and the plane of Poincaré section with a fixed Z value are shown. Intersection points (x_i, y_i), (x_{i-1}, y_{i-1})..., and intersection time t_i, t_{i-1},... are indicated. The intersection points are classified with respect to intersecting directions of the trajectory, i.e., upward (○) and downward (+) directions.

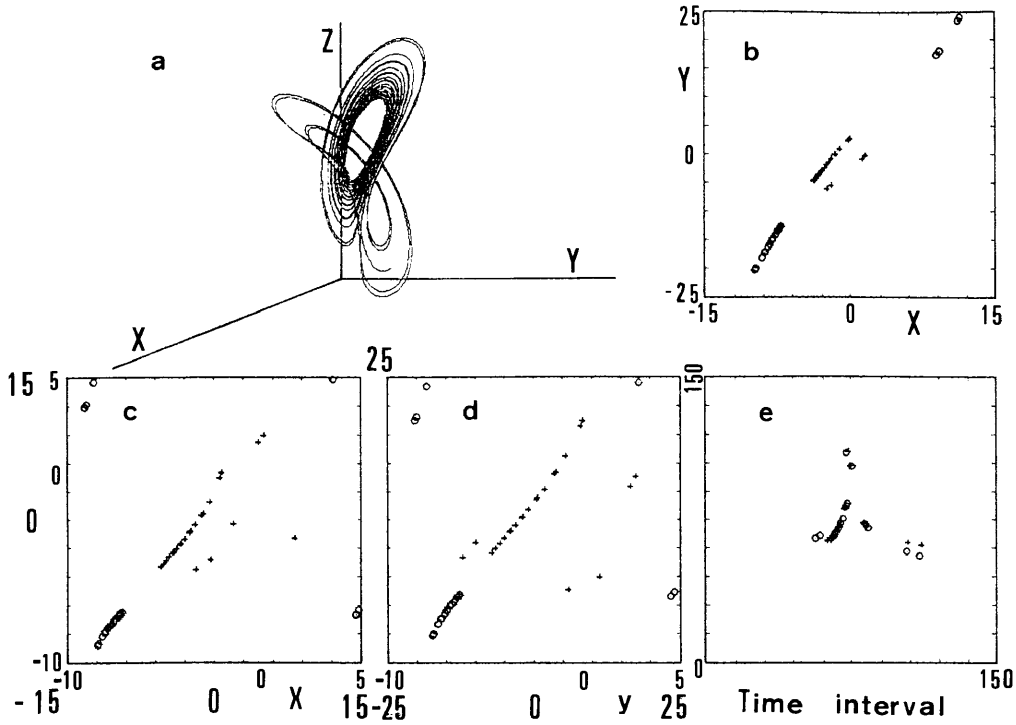

Fig. 4 Poincaré Section and Return Maps for the Lorenz Model

a: 3-d embedded manifold, b: Poincaré section at $Z=24$, c, d, e: return maps of intersecting points x and y, and of time intervals, respectively. In c and d, the two scales for the horizontal and vertical axes are indicated. The inner scale is for intersection points of the downward direction (+) and outer one for those of the upward direction (○). In e, the scales denote the iteration number of numerical calculation.

tuitive approach plays an important role. Further investigations are necessary to conclude the determinisity in the Poincaré section and the return maps.

4. Application to Economic Data

In this section we apply the embedding method to economic time series data. The economic data used here are seasonally-unadjusted and detrended quarterly data of GNP, PFCE (private final consumption expenditure), PHI (private housing investment), and IMP (import).

The two-dimensional embedding of the economic data are shown in Fig. 5 for the four pairs of economic variables, GNP-PFCE. GNP-PHI, PFCE-PHI, and PHI-IMP. It can be observed that the pairs, GNP-PFCE, GNP-PHI, and PFCE-PHI, have some structures in their embedding into 2-dimensional space, while the pair PHI-IMP has no structure.

To explore more fine structure of economic data GNP, PFCE, and PHI, the three-dimensional embedding method was applied to these data. In Fig. 6a the 3-dimensional embedded manifold of the vector time series data (GNP, PFCE, PHI) is shown. Fig. 6b shows

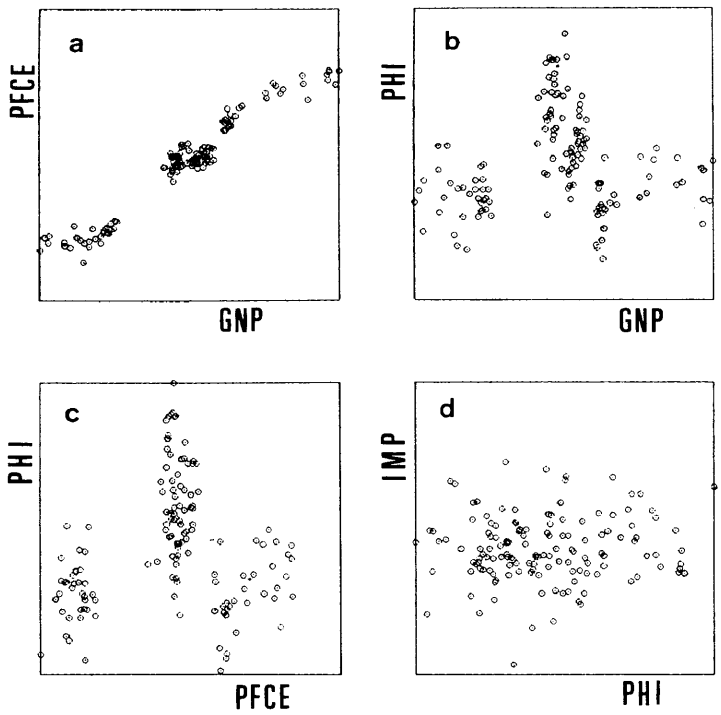

Fig. 5 Two-Dimensional Embedded Manifold of Economic Time Series.
The used data are seasonally-nonadjusted and detrended GNP, PFCE, PHI, and IMP in Japan from the second quarter of 1955 to the first quarter of 1989.

the Poincaré section at PHI=0.05. Fig. 6c and d show the return maps of intersection points with respect to GNP- and PFCE-axes, respectively. It seems possible to find the determinisity in the return maps on GNP- and PFCE-axes, if we consider only the case that the trajectory intersects the Poincaré section toward the upward direction. Fig. 6e is the retun map of time intervals between successive intersection times on the Poincaré section. Most of the time intervals distribute around four quarter, i.e., one year.

Now let us give here some comment on how the microscopic causality is approximately conserved in the macroscopic causality, when we perform the coarse-graining of the time series data. We assume here that the microscopic causality can be expressed explicitly in the following function

$$y_i=f(x_i). \tag{4.1}$$

Usually, economic data such as quarterly data are obtained by taking summation over daily or monthly data. For example, summed-up data over m periods are denoted by

$$X_j=\sum_{k=j}^{j+m-1} x_k, \quad Y_j=\sum_{k=j}^{j+m-1} y_k. \tag{4.2}$$

It is obvious that the exact relation $Y_j=F(X_j)$ cannot be obtained from the microscopic causality $y_i=f(x_i)$ except that the linear relationship, $y_i=ax_i+b$ (a and b are constants)

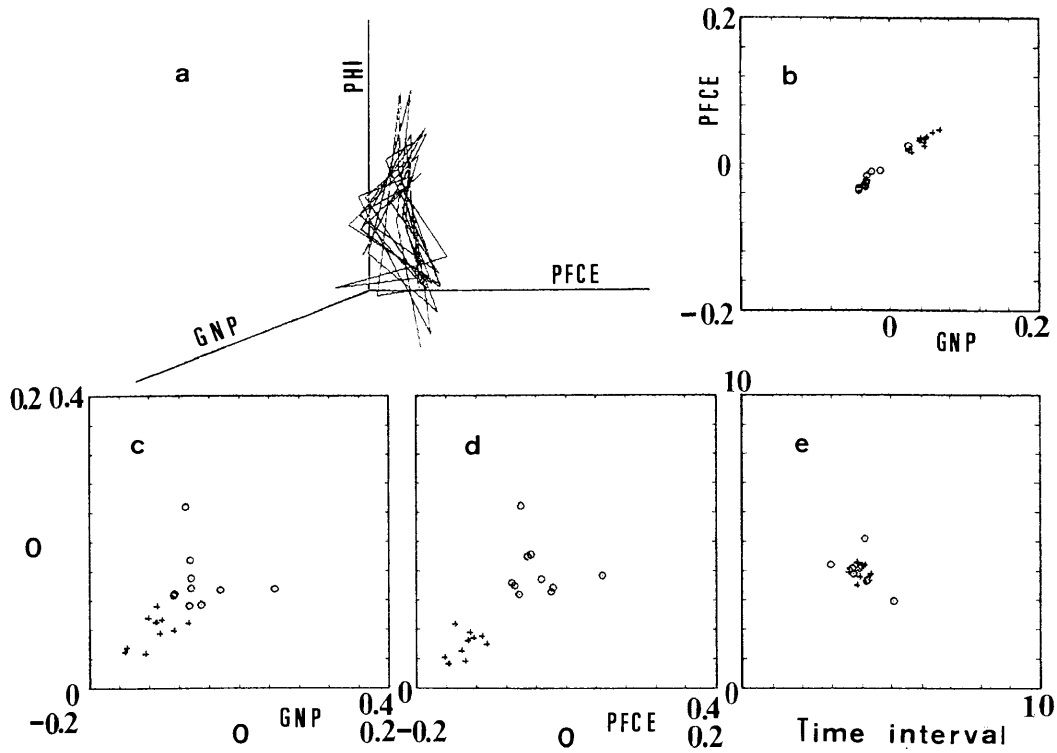

Fig. 6 3-D Embedded Manifold, Poincaré Section, and Return Maps For Seasonally-Nonadjusted and Detrended GNP, PFCE and PHI.

The data form the first quarter of 1969 to the forth quarter of 1979 in Japan are used.

a: 3-d embedded manifold, b: Poincaré section at PHI=0.05, c, d, e: return maps of intersection points on GNP and PFCE axes, and of time intervals, respectively. Inner scale in c and d is for intersection points of the downward direction (+) and outer one for those of the upward direction (○).

holds. However, the approximate relation $Y_j=F(X_j)$ are obtainable, if the microscopic causality satisfies some conditions. To obtain such conditions we carry out the following calculation. At first Y_j is written by a summation of $f(x_i)$, i.e.,

$$Y_j=\sum_{k=j}^{j+m-1} y_k=\sum_{k=j}^{j+m-1} f(x_k). \tag{4.3}$$

We also assume that the microscopic causality $f(x_k)$ can be expanded as the following power series

$$f(x_k)=a_0+a_1x_k+a_2x_k^2+a_3x_k^3+\cdots+a_lx_k^l+\cdots \tag{4.4}$$

Under this assumption we can obtain

$$\begin{aligned} Y_j=ma_0+a_1X_j+a_2\Big(X_j^2-\sum_{k}\sum_{k'}{}_{(k\neq k')}x_kx_{k'}\Big)+a_3\Big(X_j^3-\sum_{k}\sum_{k'}\sum_{k''}{}_{(k\neq k'\neq k'')}x_kx_{k'}x_{k''}\Big)+\cdots \\ +a_l\Big(X_j^l-\sum_{k}\sum_{k_1}\sum_{k_{l-1}}{}_{(k\neq k_1\neq\cdots\neq k_{l-1})}x_kx_{kl}\cdots x_{kl}\Big)+\cdots \end{aligned} \tag{4.5}$$

The right-hand side of Eq. (4.5) can be expressed as

$$f(X_j)+(m-1)a_0-g(\sum{}' x_k), \tag{4.6}$$

where $g(\sum{}' x_k)$ denotes the contribution from the higher order terms (>1) of correction. Higher-order terms correction of $g(\sum{}' x_k)$ is negligible, if $\sum x_k(1-\delta_{k,i})/\sum x_k \ll 1$ ($i \in [j, j+m-1]$), where $\delta_{k,l}$ is 1 for $k=i$ and 0, otherwise. If $\sum x_k(1-\delta_{k,i})/\sum x_k \sim 1-1/m$, the difference between Y_j and $f(X_j)+(m-1)a_0$ becomes

$$|Y_j-\{f(X_j)+(m-1)a_0\}| \sim |a_2(1-1/m)X_j^2+a_3(1-1/m^2)X_j^3+\cdots| \tag{4.7}$$

As seen from eq. (4.7), the difference between Y_j and $f(X_j)+(m-1)a_0$ becomes larger rapidly as the period m to sum up the data get larger.

According to the above calculation the condition that the coarse-grained data (or summed-up data) can conserve the microscopic causality is equal to the condition for $g(\sum{}' x_k)$ to be negligible.

5. Summary and Discussion

We have studied a method to study dynamic relationships among economic variables [10]. In that study [10], we used the three-dimensional embedding method for economic time series data. We have been considering how we can find the deterministic relation (or causality) from the time series data. We believe that the embedding method of time series data is useful to find the determinisity. However, we have few knowledge how the determinisity appears in the embedded manifold, Poincaré section and return map of intersection points on the Poincaré section. So, it is necessary to study the nature of strange attractor obtained for well-known chaotic time series data. We should also consider what condition of constraint on dynamics can be reduced from the surface intersected by the embedded manifold of time series data. These studies are carried out with the nonlinear differential equations. The embedded manifold is necessary to be classified. The goal of the study of this field is to give the method by which one can obtain a model of a set of nonlinear differential equations from the time series data actually observed.

Ackowledgments

The work was supported in part by Research Expenses in Kokushikan University (Y. N.) and Waseda University Grant For Special Research Projects (T. I.).

References

[1] J. Gleick, Chaos—making a new science, 1987 William Moris Agency Inc, New York.
H. G. Schuster, Deterministic Chaos—An Introduction, 1988, VHS, Weinheim.
[2] P. Berge, Y. Pomeau, and C. H. Vidal, L'Ordre Dans le Chaos, 1984, Hermann, Paris.
[3] B. L. Hao, Chaos, 1984, World Scientific, Singapore.

[4] C. W. Gardiner, Handbook of Stochastic Method for Physics, Chemistry and The Natural Sciences, 1983, Springer-Verlag, Berlin, Heidelberg.
[5] H. G. Van Kampen, Stochastic Processes in Physics and Chemistry, 1981, Elsevier Science Publishers, Amsterdam.
[6] E. N. Lorenz, Deterministic nonperiodic flow, J. Atmos. Sci. **20** (1963) 130–141.
[7] T. Sauer, J. A. Yorke, and M. Casdagli, Embedology, J. Stat. Phys. **65** (1991) 579–616.
[8] F. Takens, Detecting strange attractor in turbulence, Lecture Notes in Mathematics **898** (1984) 366–381.
[9] H. Froehling, J. P. Crutchfield, D. Farmer, N. H. Packard, and R. Show, On detecting the dimension of chaotic flow, Phisica **3D** (1981) 605–617.
[10] T. Inaba, Y. Nagai, and H. Wako, Dynamic relationships among economic variables examined by the embedding method, in press, 1995, Proceedings of International Conference on Dynamical Systems and Chaos 1994 in Tokyo Metropolitan University, World Scientific, Singapore.